The *SPA2* Gene of *Saccharomyces cerevisiae* Is Important for Pheromone-induced Morphogenesis and Efficient Mating

Sonja Gehrung and Michael Snyder

Department of Biology, Yale University, New Haven, Connecticut 06511

Abstract. Upon exposure to mating pheromone, *Saccharomyces cerevisiae* undergoes cellular differentiation to form a morphologically distinct cell called a "shmoo". Double staining experiments revealed that both the SPA2 protein and actin localize to the shmoo tip which is the site of polarized cell growth. Actin concentrates as spots throughout the shmoo projection, while SPA2 localizes as a sharp patch at the shmoo tip. DNA sequence analysis of the *SPA2* gene revealed an open reading frame 1,466 codons in length; the predicted protein sequence contains many internal repeats including a nine amino acid sequence that is imperfectly repeated 25 times. Portions of the *SPA2* sequence exhibit a low-level similarity to proteins containing coiled-coil structures. Yeast cells containing a large deletion of the *SPA2* gene are similar in growth rate to wild-type cells. However, *spa2* mutant cells are impaired in their ability to form shmoos upon exposure to mating pheromone, and they do not mate efficiently with other *spa2* mutant cells. Thus, we suggest that the SPA2 protein plays a critical role in cellular morphogenesis during mating, perhaps as a cytoskeletal protein.

CELLULAR morphogenesis is a fundamental process in eukaryotes. As cells differentiate, asymmetric cell growth often ensues to form distinct cell types and shapes. Well-known examples in multicellular organisms include neuronal cells, in which long projections grow from the cell body, and epithelial cells.

Yeast cells undergo polarized cell growth at two times in their life cycle, during normal mitotic growth and before mating. In late G1 of the cell cycle, bud emergence begins at one site on the edge of the cell. Cell growth occurs principally at the tip of the bud until cytokinesis. Before mating, yeast cells also undergo morphogenic differentiation that involves asymmetric cell growth (Byers, 1981; Baba et al., 1989). Upon exposure to appropriate mating pheromones, cells arrest in G1; a projection then emerges from one edge of the cell to form a pear-shaped cell called a "shmoo". Contact between two mating cells occurs at the outgrowth (for a review on mating see Cross et al., 1988).

Genetic screens and studies of cytoskeletal proteins have revealed a number of components that are thought to participate in polarized cell growth and morphogenesis in yeast. Chitin, actin, and two actin binding proteins, SAC6 and ABP1 (Adams and Pringle, 1984; Kilmartin and Adams, 1984; Adams et al., 1989; Drubin et al., 1988), all accumulate at the incipient site of bud formation (Drubin, 1990). As the bud enlarges, actin, SAC6, and ABP1 concentrate as spots within the bud near its surface, while chitin remains at the bud neck. Some of the actin and SAC6 protein remain behind in the mother cell as spots and cables. The *CDC3*, *CDC10*, and *CDC12* gene products also accumulate at the site of bud formation (Kim, H. B., B. K. Haarer, and J. R. Pringle, personal communication). These proteins are thought to be components of 10-nm filaments that surround the bud neck; like chitin, they also remain as a ring around the bud neck as the bud enlarges (see Haarer and Pringle, 1987).

Three other genes, *CDC24*, *CDC42*, and *CDC43*, were identified through genetic screens and are important in budding (Hartwell et al., 1974; Pringle and Hartwell, 1981). Cells with mutations in any of these genes continue to grow and undergo nuclear division, but they are defective in bud emergence and accumulate as unbudded, multinucleate cells. From DNA sequence analysis, the CDC24 protein is predicted to be a calcium binding protein (Ohya et al., 1986*a*,*b*), while the *CDC42* gene product is homologous to the RAS and RHO GTP binding proteins of yeast and other eukaryotes (Johnson and Pringle, 1990).

Shmoo morphogenesis has not been as well-characterized at a molecular level, and consequently less is known concerning the cytoskeletal and other components that are important for this process. During shmoo differentiation the nucleus migrates to the base of the shmoo projection and the spindle pole body (SPB),[1] the microtubule organizing center of yeast, is oriented toward the shmoo tip (Hasek et al., 1987; Baba et al., 1989). Actin spots concentrate in the region of the shmoo apex (Hasek et al., 1987), and three other proteins, a agglutinin (Watzele et al., 1988), which is involved in agglutination, the FUS1 protein (Trueheart et al.,

1. *Abbreviation used in this paper*: SPB, spindle pole body.

1987), which is involved in cell–cell fusion, and the SPA2 protein (described below) are the only other proteins that have been identified which specifically localize to the region of shmoo growth.

The SPA2 protein resides at sites of polarized cell growth in both mating and nonmating yeast cells (Snyder, 1989). In budded yeast cells of **a**, α, or **a**/α mating type, the SPA2 protein resides at the tip of the bud. In unbudded cells, it forms a small patch located on one edge of the cell, and the SPA2 localization region is probably the site of bud emergence (Snyder, 1989). The SPA2 protein is also polarized in mating yeast cells; in **a** cells treated with α-factor, the SPA2 protein resides at the tip of the shmoo. The *SPA2* gene has been disrupted with both insertion mutations and a deletion mutation; *spa2* mutants grow well but appear slightly rounder than their wild-type counterparts. Moreover, whereas wild-type cells select a new bud site at a specific location relative to the previous site, the budding patterns of *spa2* mutants are slightly disrupted. Thus, in addition to serving as a marker for sites of polarized cell growth, the SPA2 protein is involved in polarized cell division.

Described below are studies to further investigate the role of the *SPA2* gene in yeast cell growth. The nucleotide sequence of the *SPA2* gene was determined; portions of the predicted protein sequence are similar to that of proteins that form coiled-coil structures. Disruption of the *SPA2* gene indicates that the SPA2 protein is important for pheromone-induced morphogenesis and mating.

Materials and Methods

Yeast Strains and General Methods

All yeast strains are derived from S288C and are congenic; a strain list is presented in Table I. General genetic manipulations and growth media are described by Sherman et al. (1986). General cloning procedures are described by Davis et al. (1980) and Sambrook et al. (1989).

DNA Sequence Analysis

SPA2 clones were described by Snyder (1989). The sequence of the *SPA2* gene was determined by the dideoxy chain termination method of Sanger et al. (1977). Sequence analysis was determined from both strands; in areas of ambiguity, multiple subclones were prepared and analyzed. Nested deletions prepared by subcloning, "shotgun" cloning of random fragments from digests of restriction enzymes with four bp recognition sequences, and specific restriction fragments were analyzed to determine the DNA sequence (Sambrook et al., 1989). Computer analysis of the DNA sequence and the predicted protein sequence was performed using the FASTA programs (Pearson and Lipman, 1988; Pearson, 1990) or the DNA Strider programs (Christian Marck, Service de Biochimie, Centre d'Etudes Nucleaires de Saclay 91191 Gif-sur-Yvette, Cedex, France). Searches of the NBRF data bank were performed with the FASTA programs (Pearson, 1990), and GenBank searches were with both the FASTA and tFASTA programs (Pearson, 1990). All searches were performed using ktup = 2 (see Pearson, 1990). Comparison of the predicted SPA2 protein sequence with itself (see Fig. 2) was performed using the plFASTA program and a ktup value of 2 (Pearson, 1990). The significance of the sequence similarity between the SPA2 protein and the keratin genes was checked using the RDF2 programs (Pearson, 1990); the optimized sequence is greater than five standard deviations above the mean of the shuffled scores, indicating the sequence similarity is statistically significant.

Construction and Analysis of the spa2-Δ2::TRP1 and spa2-Δ3::URA3 Disruption Mutants

To construct the *spa2-Δ3::URA3* allele, a 6.7-kb Sal I/Hind III fragment containing the *SPA2* gene (see Fig. 1) was subcloned into YCp50 (Johnston and Davis, 1984). The resulting plasmid is called p203. p203 was digested with Sac I and Sph I and ligated to a 1.1-kb Hind III fragment containing the *URA3* gene. Before ligation, both DNAs were treated with the large fragment of *E. coli* DNA polymerase I in the presence of dNTPs. To construct *spa2-Δ2::TRP1*, the p188 plasmid containing the *spa2-Δ1::TRP1* allele (Snyder, 1989) was cleaved with Sac I and partially digested with Stu I which cuts in the *TRP1/ARS1* fragment. After treating the ends with the large fragment of *E. coli* DNA polymerase I as described above, the appropriate fragment was purified from an agarose gel, ligated, and transformed into *E. coli*. The final plasmid contains a 0.8-kb Eco RI/Stu I *TRP1* fragment in place of the 3.5-kb Sac I/Sph I region of *SPA2*.

Linear DNA fragments of each of the *spa2* alleles were transformed into the diploid yeast strain Y270 (Ito et al., 1983; Rothstein, 1983), and the resulting heterozygotes were sporulated. Three transformants were sporulated for each allele. Most of the dissected tetrads yielded four viable spores; in these tetrads, the *TRP1* or *URA3* marker segregated $2^+:2^-$. Proper substitution at the *SPA2* locus was determined by three criteria: (*a*) gel blot analysis of genomic DNA using ^{32}P-labeled *SPA2* probes (Snyder and Davidson, 1983; Feinberg and Vogelstein, 1983); (*b*) failure of the *spa2* mutant cells to stain with anti-SPA2 antibodies; and (*c*) 2:2 segregation of the *TRP1* and *URA3* markers from *spa2-Δ3::URA3/spa2-Δ2::TRP1* heterozygotes.

Analysis of budding patterns of new haploid and diploid cells was as described by Snyder (1989). The results for haploid mothers, diploid mothers,

Table I. Strain List

Y601	*MATα ura3-52 lys2-801 ade2-101 trp1-901 his3-Δ200 spa2-Δ3::URA3*
Y602	*MATa ura3-52 lys2-801 ade2-101 trp1-901 his3-Δ200 spa2-Δ3::URA3*
Y603	*MATα ura3-52 lys2-801 ade2-101 trp1-901 his3-Δ200*
Y604	*MATa ura3-52 lys2-801 ade2-101 trp1-901 his3-Δ200*
Y609	*MATa ura3-52 lys2-801 ade2-101 trp1-901 his3-Δ200 spa2-Δ2::TRP1*
Y610	*MATα ura3-52 lys2-801 ade2-101 trp1-901 his3-Δ200*
Y611	*MATα ura3-52 lys2-801 ade2-101 trp1-901 his3-Δ200*
Y612	*MATa ura3-52 lys2-801 ade2-101 trp1-901 his3-Δ200 spa2-Δ2::TRP1*
Y431F$^-$	*MATa ura3-52 lys2-801 ade2-101 trp1-901 leu2-Δ98*
Y196	*MATα trp1 ρ°*
Y197	*MATa ura3-52 lys2-801 ade2-101 trp1-901 his3-Δ200 spa1-2::URA3*
Y270 (YNN318)	*MATa ura3-52 lys2-801 ade2-101 trp1-901 his3-Δ200*
	MATα ura3-52 lys2-801 ade2-101 trp1-901 his3-Δ200
Y650	*MATa ura3-52 lys2-801 ade2-101 trp1-901 his3-Δ200 spa2-Δ2::TRP1*
	MATα ura3-52 lys2-801 ade2-101 trp1-901 his3-Δ200 spa2-Δ3::URA3
7440-1	*MATa ura3-52 cry1 lys2° ade2-1° SUP4-3^{ts} his4-580^a trp1^a leu2-3,112 ste2-T326*
7413-3-3	*MATa ura3-52 cry1 lys2° ade2-1° SUP4-3^{ts} his4-580^a trp1^a leu2-3,112 tyr1° STE2*

All strains are in an S288C congenic background, except for 7413-3-3 and 7440-1 which are in an A364A background. The two sets of strains, Y601-Y604 and Y609-Y612, are each the progeny of a single meiosis of a Y270 transformant heterozygous for the *spa2* deletion allele.

and diploid daughters were determined by observation of strains Y602 (*spa2*), Y604 (*SPA2*), Y270 (*SPA2/SPA2*), and Y650 (*spa2/spa2*). Between 33 and 74 cells were observed in each case. *R* values which are the ([number of divisions <90° from the old bud site or birth scar]−[number of divisions <90°])/(total number of divisions) provide a measure of axial or polar budding (Snyder, 1989). For 100% axial budding $R = 1.00$, for random budding $R = 0.00$, and for 100% polar budding $R = -1.00$. *R* values were as follows: (haploid mothers) *SPA2* ($n = 33$), 1.00 *spa2* ($n = 37$), 0.90; (diploid mothers) *SPA2/SPA2* ($n = 39$), 0.49 *spa2/spa2* ($n = 43$), 0.26; (diploid daughters) *SPA2/SPA2* ($n = 68$), −0.56 *spa2/spa2* ($n = 74$), −0.70. These results are comparable to those published for *spa2-Δ1*. The results for haploid daughters were not determined for technical reasons.

Mating Tests, Cytoduction Tests, and Agglutination Assays

For high density mating experiments, a culture of yeast cells growing exponentially in YPD was incubated until OD (600) = 0.4. 2×10^6 cells (0.5 ml) of the experimental mating strain (listed first in Table II) was mixed with 4×10^6 cells (1 ml) of the tester strain. Cultures were then allowed to stand in an upright 18-mm test tube without shaking at 30° and cells settled to the bottom of the tube. After incubation for 4 h, cultures were vortexed vigorously and serial dilutions were plated on selective yeast minimal plates to determine the number of diploids. Greater than 200 cells were scored for each sample. The results presented in Table II are for ρ^+ strains; similar relative efficiencies were observed when the experimental mating strain was ρ°. For wild-type strains, 25–47% of the experimental cells had mated.

Mating experiments were also carried out at low cell densities. Cultures of yeast cells growing exponentially in YPD were incubated until OD (600) = 0.3. 7.5×10^4 *MATa* cells (2.5 μl) were mixed with 7.5×10^4 *MATα* cells (2.5 μl) in 50 μl of water, and immediately spread on 90-mm yeast minimal plates that select for diploid cells. The cell density is estimated to be in the range of 23–46 total cells/mm^2 and the mating efficiency of wild-type cells was ~0.3%. Some variation in the mating efficiencies was observed under these conditions; we suspect that one source of the variation was the variable rate with which different plates absorbed the exogenous solution; the longer the period of absorption, the higher the mating efficiency, perhaps due to the ability of cells to clump while still suspended in liquid media. Therefore, plates of similar age (and therefore similar moisture content) were used for each experiment.

For cytoductant tests, the experimental mating strains were ρ° and the conditions were similar to those of the high density mating assays. Platings were performed on appropriate yeast minimal plates containing glycerol plus 0.02% glucose that allow only diploids and cytoductants to grow. Cytoductants and diploids were subsequently identified by patching individual colonies and then mating to a set of mating-type tester strains. The patches that fail to mate are assumed to be diploid; this was confirmed for 10 random diploids chosen from each cross by the appearance of tetrads when incubated in sporulation medium. The patches that mate should reflect the number of haploid cytoductants. (Note that *spa2* mutants do not lose chromosomes as assayed using chromosome fragments [data not shown; tests are described in Hieter et al., 1985; Snyder and Davis, 1988].) As further evidence that the cytoductants were properly scored, four cytoductant colonies from the *spa2* × *spa2* matings in Table III were mated to mating tester strains and sporulated. Four viable spores were produced, as expected. Control experiments using ρ° *spa1* mutant cells (Y197; Snyder and Davis, 1988) yield cytoductant to diploid ratios of 0.92 when mated with Y196. We note that this cytoductant assay, like other assays using can^R markers (Conde and Fink, 1976), probably underestimates the actual number of cytoductants because the cytoductants have the opportunity to remate. To partially alleviate this concern, we determined whether the cytoductant/diploid ratios might change with respect to mating incubation times. Cytoductant/diploid ratios were found to be similar for cells mated for four hours relative to cells mated for 7.5 h.

Agglutination assays were carried out similar to those described by Hartwell (1980). 1 ml of a *MATa* culture at 3×10^6 cells/ml was mixed with 1 ml of a *MATα* culture at the same density. Cells were incubated with shaking for 1 h at 30°. Cells were then pelleted in a microcentrifuge at 735 *g* for 5 min. They were gently mixed to resuspend the clumps and then allowed to stand for 15 min which allows the agglutinated cells to settle. The OD (600) of the supernatant was then determined and compared with cultures containing two *MATa* strains and two *MATα* strains. For the wild-type and the *spa2* matings, no difference was observed in their ability to agglutinate in two separate experiments.

Mating Factor Arrest, Immunofluorescence, and Actin Staining Experiments

5-ml cultures of *spa2* (Y602 and Y609) and wild-type (Y604) yeast cells were grown in YPD media at 30° to OD (600) = 0.3. α-factor (Sigma Chemical Co., St. Louis, MO) was added to a final concentration of 4.0 μg/ml. After incubation for 50 min at 30° the treatment was repeated and cells were incubated for an additional 45 min. 0.6 ml of a 37% formaldehyde solution was added and the culture was allowed to shake for 1 h at room temperature. Cell morphology was then examined using a light microscope.

For immunofluorescence experiments, formaldehyde-treated cells were washed three times with 1.3 M sorbitol, 50 mM KPO_4, pH 6.8 (solution A), and resuspended in 400 μl of solution A. Spheroplasts were prepared by mixing 200 μl of cells with 200 μl of solution A containing 5 mg/ml zymolyase 100T, 0.03% glusulase, and 0.2% beta-mercaptoethanol, and incubating at 37° for 1 h. Cells were washed once and placed on polylysine-coated slides. The slide-bound cells were washed three times with PBS (150 mM NaCl, 50 mM $NaPO_4$, pH 7.2) containing 0.1% BSA.

Immunofluorescence was performed with affinity-purified, anti-SPA2 antibodies as described by Adams and Pringle (1984), Kilmartin and Adams (1984), and Rose and Fink (1987). For double immunofluorescence with rat antitubulin and rabbit anti-SPA2 antibodies (YOL1/34; Kilmartin et al., 1982), the second antibodies were Texas red-conjugated goat antirabbit antibodies (Amersham Corp., Arlington Heights, IL), and fluorescein-conjugated goat antirat antibodies (Cappel Laboratories, Malvern, PA).

Actin/SPA2 double staining experiments were performed similar to those described by Adams and Pringle (1984). Samples, prepared as above, were incubated overnight with PBS/BSA (PBS + 0.1% BSA) containing affinity-purified anti-SPA2 antibody and 80 μg/ml rhodamine-conjugated phalloidin (Molecular Probes Inc., Eugene, Oregon). Cells were washed three times with PBS/BSA containing 2 μg/ml phalloidin (PBS/BSA/phalloidin solution), and incubated in the PBS/BSA/phalloidin solution containing fluorescein-conjugated goat antirabbit antibodies (20 μg/ml; Cappell) for 20 min. Cells were then washed three times in PBS/BSA/phalloidin solution and once in PBS/BSA without phalloidin. Mounting solution consisting of 70% glycerol, PBS, 2% n-propyl gallate, and 0.25 μg/ml Hoechst 33258 was added and samples were viewed using a fluorescence microscope. Identical results for each of these studies were obtained for the Y602 and Y609 *spa2* mutant strains.

Results

Construction of a Large Deletion Mutation of the SPA2 Gene

Previous studies of *SPA2* function have utilized two insertion mutations and a partial deletion (*spa2-Δ1*). Strains carrying the *spa2-Δ1* deletion mutation are still capable of making approximately one third of the wild-type gene product and thus may have some level of *SPA2* function. To address this possibility and to determine the null phenotype, we used the DNA sequence information presented below to construct two new alleles, *spa2-Δ2::TRP1* and *spa2-Δ3::URA3*, in which a 3,500-bp segment of the *SPA2* gene was replaced with the *TRP1* and *URA3* genes, respectively (Fig. 1). These mutant genes contain only 39 codons of *SPA2* sequence upstream of the selectable marker. Each of these alleles was introduced into diploid yeast strains by transformation. Sporulation of the resulting heterozygotes yielded four viable spores; the selectable marker segregated 2+:2− indicating that the *SPA2* gene is not essential for cell growth and viability.

spa2-Δ2::TRP1 and *spa2-Δ3::URA3* mutants grow at the same rate as wild-type, and mutant cells appear marginally rounder than their wild-type counterparts. Diploid *spa2* mutants also undergo meiosis successfully to form tetrads with four viable spores. *spa2* asci frequently contain a bud adjacent to the four-spored ascus indicating that the cells had not arrested properly before the entry into meiosis. As might be

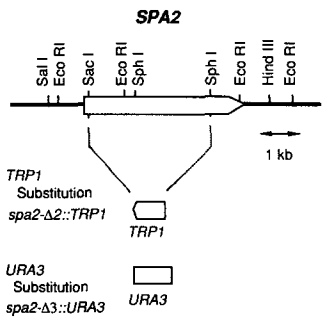

Figure 1. Deletion/substitution mutations in the *SPA2* gene. A 3,500-bp fragment of the *SPA2* gene was replaced with an 800-bp *TRP1* fragment to create *spa2-Δ2::TRP1*. The same region of *SPA2* was replaced with a 1.1-kb *URA3* fragment to create *spa2-Δ3::URA3*. The direction of the *TRP1* fragment indicates the orientation of that gene.

expected if the *SPA2* gene product is involved in budding, the budding patterns of *spa2* mutants are slightly disrupted from those of wild-type cells (see Materials and Methods). All of these phenotypes are the same as those noted previously for the *spa2-Δ1* mutation.

The SPA2 Gene Is Important for Efficient Mating

The greatest defect of the *spa2-Δ2::TRP1* and *spa2-Δ3::URA3* mutations is in conjugation, and the severity of the defect depends upon the cell densities of the mating strains (see Material and Methods). When *spa2* mutant cells are mated with other *spa2* mutants at high cell densities, diploids form at 1.0–2.0% the frequency of wild-type cells (Table II). At lower cell densities, the *spa2* conjugation defect is even greater (see Materials and Methods); *spa2/spa2* diploids form at <0.1% the frequency of wild-type diploids.

The mating defect is most severe when both mating partners carry an *spa2* mutation. When *spa2* cells of either mating type are mated with wild-type cells at high density, a zero- to fourfold decrease in mating efficiency is observed, as compared to matings between wild-type cells. When mated at low cell densities, a sixfold or greater decrease is observed. Thus, *spa2* mutants are defective in mating, and the defect is strongest when *spa2* cells are mated with other *spa2* mutant cells and under conditions of low cell densities.

Table II. Relative Mating Efficiencies of spa2 Mutant Cells

Mating strain	Tester strain	Relative efficiency: high cell density	Relative efficiency: low cell density	Strains
wt	wt	1.0	1.0	Y603 × Y431F⁻
spa2	wt	0.73	0.16	Y601 × Y431F⁻
wt	*spa2*	0.23	NA	Y431F⁻ × Y601
spa2	*spa2*	0.013	<0.001	Y609 × Y601
spa2	*spa2*	0.018	NA	Y601 × Y609
spa2	wt	NT	1.0 (0.18)*	Y601 × 7413-3-3
spa2	*ste2-T326*	NT	0.17 (0.03)*	Y601 × 7440-1

Relative mating efficiencies of *spa2* mutant cells at two different cell densities. For the high cell density mating experiments, a twofold excess of tester cells listed in the second column was incubated with the cells listed in the first column as described in Materials and Methods. Serial dilutions were plated to select for diploids. The relative number of diploids reported is from an average of three experiments. Similar results were obtained using other possible pairwise crosses between *spa2* mutant and wild-type cells. For the low cell density mating experiments equal numbers of mating partners were mixed together and immediately spread over a large surface area (see Materials and Methods). For *spa2* cells mated with *spa2* cells no diploids were observed (in five independent experiments). The <0.001 frequency is estimated from the fact that >1,200 wild type diploids would have formed under similar experiments. *NA*, not applicable; *NT*, not tested.

* Note the 7413-3-3 and 7440-1 strains are derived from a different yeast background (A364A) than the other strains (S288C); therefore, the values provided are relative to each other. The values in parenthesis are relative to the wt X wt matings in line 1, which were performed in parallel.

spa2 Mutants Have Defects in Pheromone-induced Cell Morphogenesis

There are several possible explanations for the *spa2* mating defect. These include defects in (*a*) proper cell cycle arrest; (*b*) agglutination; (*c*) morphological changes; (*d*) cell wall breakdown/cytoplasmic fusion; and (*e*) nuclear fusion (karyogamy).

To determine whether any of the early mating steps were blocked in *spa2* mutants, we examined whether mutant cells arrested properly upon exposure to mating pheromone. Wild-type and *spa2* mutant *MATa* cells were incubated with α-factor for 95 min and then examined in the light microscope. As shown in Figs. 2 and 3, >98% of both *spa2* and wild-type cells were arrested. Staining with Hoechst 33258 revealed a single nucleus in every unbudded cell. However, the cell morphology was strikingly different between *spa2* and wild-type cells. 84% of wild-type cells had formed recognizable shmoos, and the majority of these had very pointed projections (Figs. 2 and 3). In contrast, only 12% of the *spa2* mutant cells appeared shmoo-like, and these typically had smaller, rounded projections. Although the *spa2* cells were not dividing as evidenced by lack of buds, the optical density of the culture increased at an equivalent rate to that of wild-type cells, suggesting that the cells continued to grow over the course of this experiment.

The morphological defect of *spa2* cells is not restricted to *MATa* cells. *spa2 MATa* cells were incubated with *spa2 MATα* cells and examined in the light microscope. Most of the cells had arrested, but few shmoo-like cells were present as compared with wild-type mating cells where many cells formed shmoos (not shown). Therefore, both *MATa* and *MATα* cell-types appear to be defective in shmoo formation. Thus, *spa2* mutants are able to arrest properly, but they do not undergo the morphological changes characteristic of wild-type cells.

spa2 Mutant Cells Appear Normal in Agglutination and Have a Slight Defect in Nuclear Fusion

Other aspects of the mating process were also examined. Mating cultures of *spa2* mutant cells agglutinate at levels similar to that of wild-type cells, indicating that the adhesion response is normal (data not shown; see Materials and Methods).

If the SPA2 protein is a cytoskeletal component (see below), particularly one involved in cell polarity, it is plausible that many cells might be able to undergo cytoplasmic fusion properly, but have difficulty in nuclear fusion. Nuclear fusion relies on proper orientation of the two nuclei such that their spindle pole bodies face one another; the interdigitating microtubules that emanate from the spindle pole bodies then enable the two nuclei to come together and fuse (Byers, 1981). Defects in cell polarity might be expected to disturb the nuclear orientation process and subsequently lead to nuclear fusion defects.

We therefore tested whether *spa2* mutants can still fuse their cytoplasm properly, but fail to undergo nuclear fusion.

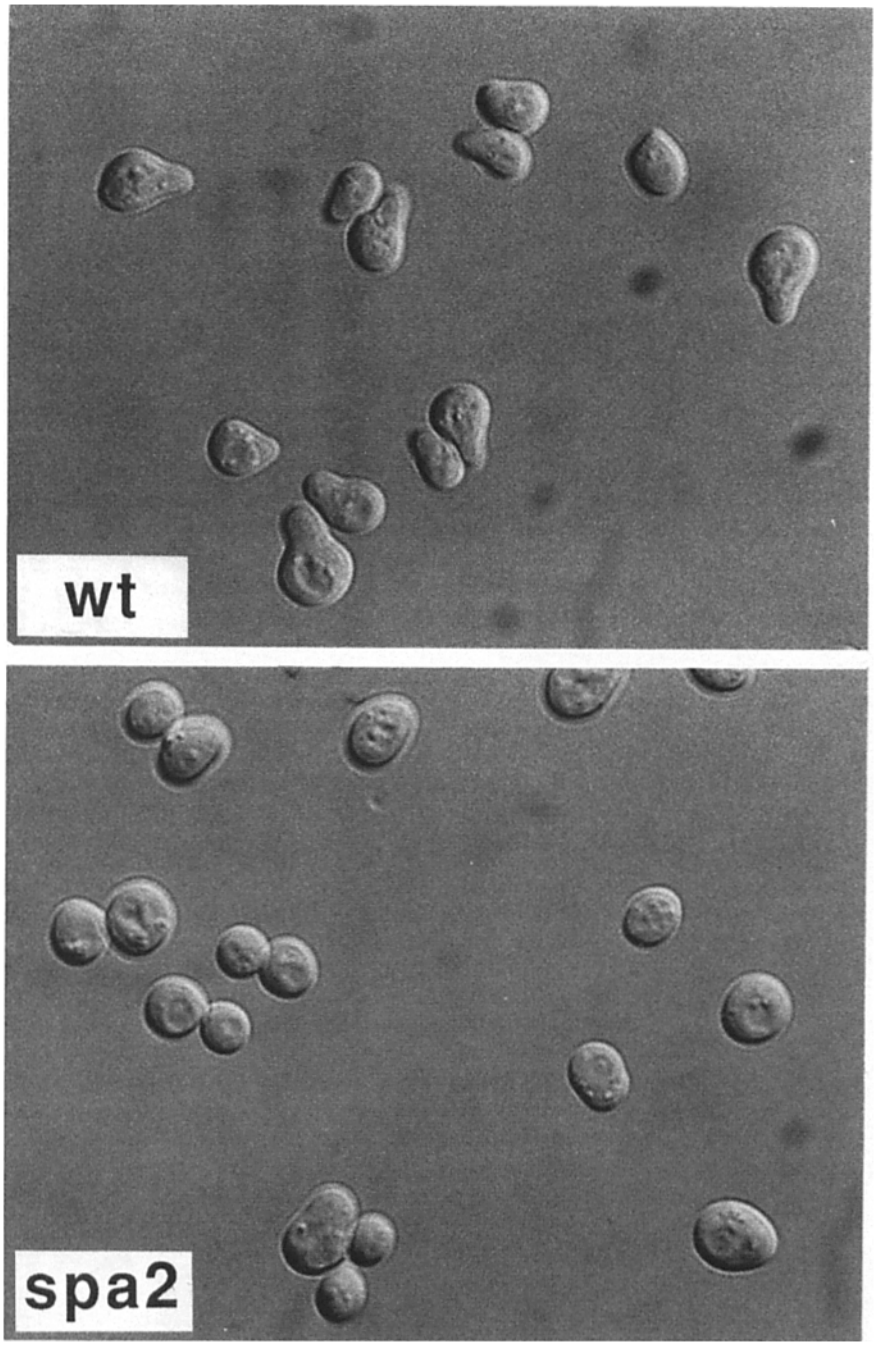

Figure 2. Comparison of wild-type (Y604) and *spa2* mutant (Y602) cells treated with mating pheromone. *MATa* cells were treated with α-factor as described in Materials and Methods, fixed, and viewed using differential interference microscopy. The majority of wild-type cells form shmoos with pointed projections. In contrast, most of the *spa2* mutant cells are round or oval; occasionally a shmoo-like cell with a rounded projection is observed such as the one near the bottom of the field.

A defect specifically in karyogamy would lead to a mixing of cytoplasm and formation of a heterokaryon; heterokaryons are unstable and produce haploid progeny (called cytoductants, for transfer of cytoplasm). Using the genetic tests described in Materials and Methods, we tested whether *spa2* mutant cells form cytoductants at a high frequency compared to the frequency at which they form diploids. Table III demonstrates that although there is a substantial increase in the number of cytoductants that form during mating of *spa2* mutants, this increase alone is not enough to account for the overall 50–100-fold mating defect observed under similar mating conditions.

Actin and Tubulin in Wild-type and spa2 Mutant Cells Treated with α-factor

To further understand the nature of the morphological defect in *spa2* mating cells, we examined the subcellular distribution of two cytoskeletal proteins, actin and tubulin, in both wild-type and *spa2* mutant cells. Actin has been previously shown to have an asymmetric distribution in cells that are preparing to mate (Hasek et al., 1987). The subcellular distribution of the SPA2 protein was first compared with that of actin in wild-type cells by treating *MATa* cells with α-factor and staining the resulting shmoos with both anti-SPA2

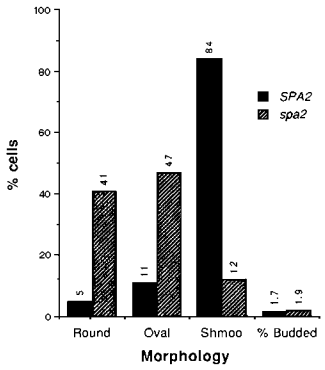

Figure 3. Summary of cell morphologies after exposure to mating pheromone. Wild-type and *spa2 MATa* yeast cells were incubated in the presence of α-factor as described in Materials and Methods. The number of unbudded cells with round, oval, and shmoo or shmoo-like morphology was determined by counting 400 unbudded cells. The percentage of budded cells was determined by counting 363 and 425 cells for Y604 and Y602 cells, respectively.

Table III. Cytoductant Tests

Mating strain	Tester strain	Cytoductant/ diploid ratio	*n*	Strains
wt	wt	0.00	637	Y603 ρ° × Y431
wt	wt	0.00	238	Y431 ρ° × Y603
spa2	wt	0.00	208	Y601 ρ° × Y431
wt	*spa2*	0.011	183	Y431 ρ° × Y601
spa2	*spa2*	0.078	262	Y609 ρ° × Y601
spa2	*spa2*	0.043	185	Y601 ρ° × Y609

A twofold excess of ρ^+ cells was incubated with the ρ° cells at high density as described in Materials and Methods. Serial dilutions were plated on glycerol plates that allow both diploids and cytoductants to grow; diploids and cytoductants were distinguished in subsequent tests (see Materials and Methods). *n*, total number of diploids plus cytoductants scored.

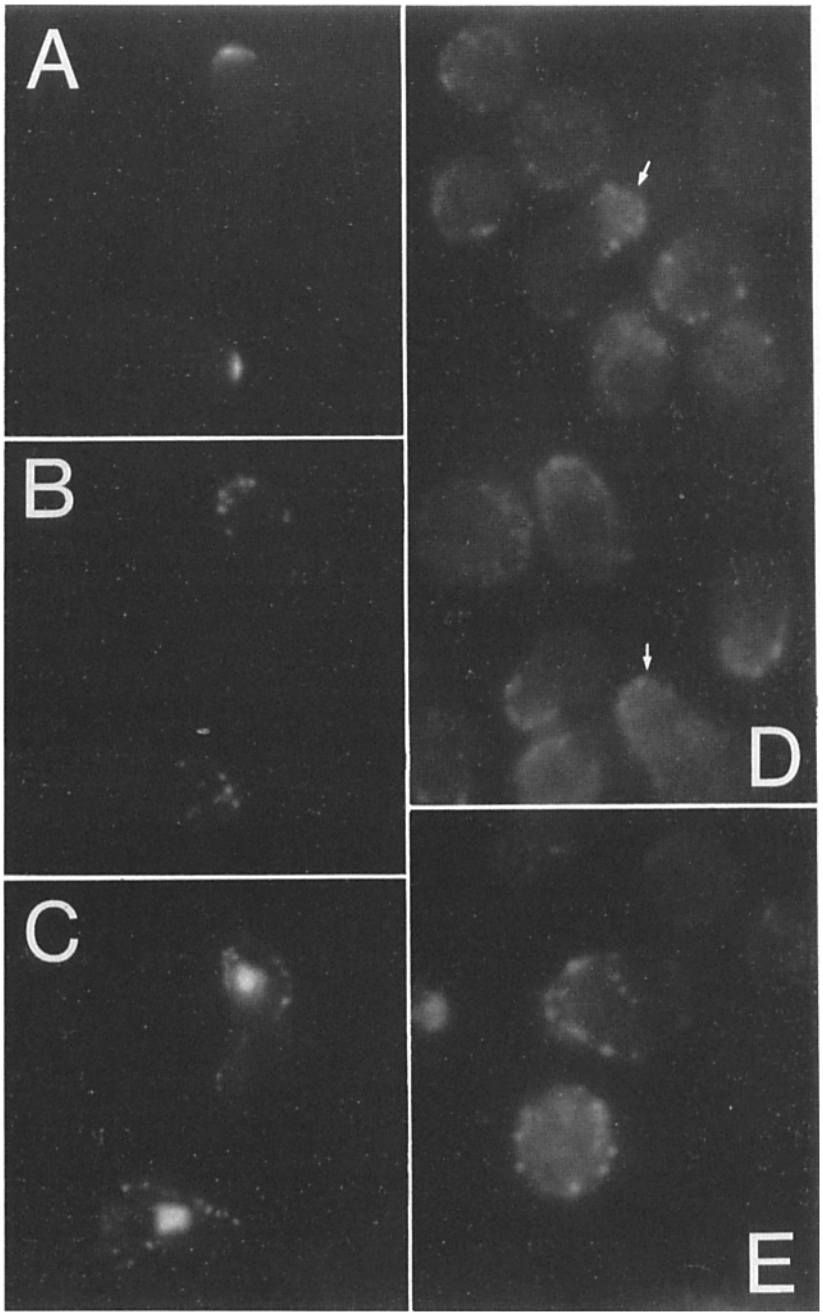

Figure 4. Actin and SPA2 labeling of yeast cells treated with mating pheromone. *MATa* yeast cells were arrested with mating pheromone and double stained using affinity-purified SPA2 antibodies and rhodamine-conjugated phalloidin which binds F actin. (*A–C*) The same wild-type cells (Y604) stained with anti-SPA2 antibodies (*A*), phalloidin which binds F actin (*B*), or Hoechst 33258 (*C*). For *B*, faint staining of the actin cables was apparent in the bottom cell, but is difficult to see in the figure. Note that the nucleus has moved near the projection (*bottom cell*) or within it (*top cell*). (*D* and *E*) parallel experiments using *spa2* mutant cells (Y602). Only the phalloidin stains are shown; anti-SPA2 antibodies failed to label. Note that round cells exhibit staining near the surface randomly around the cell, whereas oval cells typically stain preferentially near one end. The shmoo-like cells indicated by small arrows stain at the end of the projection. The field shot in panel D is ~85% the magnification of the other panels.

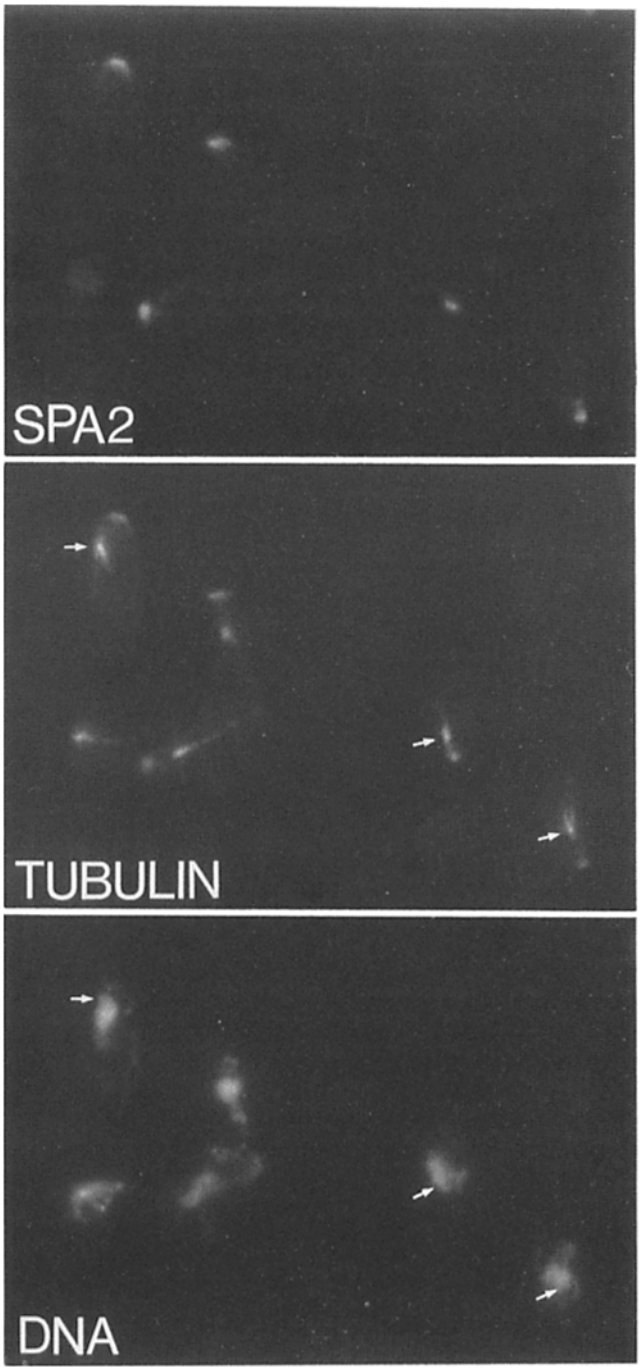

Figure 5. SPA2/tubulin double immunofluorescence of yeast cells treated with mating pheromone. Wild-type yeast cells (Y604) were treated with α-factor and double stained with affinity-purified anti-SPA2 antibodies (*top panel*) and YOL1/34 an antitubulin antibody (*middle panel*). Cells were also stained with Hoechst 33258 to visualize the DNA (*bottom panel*). The SPA2 signal was quite intense and some crossover of signal is present in the tubulin panel. For all the cells shown in the figure, the inferred position of the spindle pole body (indicated by an arrow for some of the cells) is on the side of the nucleus facing the shmoo tip (and SPA2 staining region).

antibodies and rhodamine-conjugated phalloidin, which binds filamentous actin (F actin). As shown in Fig. 4, phalloidin binding is localized in spots, which accumulate in the shmoo projection and are particularly concentrated at the shmoo tip. The majority of these spots are located at the cell periphery. Faint actin cables, which are difficult to see in the figure, and a few spots are sometimes observed in the main part of the cell. In contrast, the SPA2 protein is sharply localized to a well-defined region at the shmoo tip.

To determine whether actin displays a polarized distribution in *spa2* cells treated with pheromone, phalloidin staining experiments were performed on *spa2* mutant cells in parallel with the wild-type staining experiments. In *spa2* cells, the actin spots were usually present near the cell surface, as was found for wild-type cells (Fig. 4). However, the staining varied depending upon the shape of the cell. The majority of round cells (80%) had actin spots distributed randomly around the cell. Most oval cells (80%) exhibited actin polarity with the spots located near one end of the oval. The shmoo-like cells also showed a polarized distribution of actin towards the shmoo tip. Thus, actin polarity is maintained in oval and shmoo-like cells, but is disrupted in the round cells.

The location of intracellular microtubules in pheromone-treated cells was also examined by staining with an antitubulin antibody, YOL1/34. In wild-type mating cells, the nucleus migrates to the neck of the projection (Baba et al., 1989; Hasek et al., 1987; Figs. 4 and 5). The SPB is on the side of the nucleus facing the shmoo tip. Usually, one or more long microtubule bundles extend back from the SPB toward the main part of the cell (Fig. 5). In many cells, a single microtubule bundle is also observed extending toward the shmoo tip and intersecting the SPA2 staining region. In *spa2* mutant cells, the SPB/nucleus orientation is maintained in the shmoo-like cells and the oval cells (not shown). In the shmoo-like cells, the SPB lies towards the tip of the projection, in oval cells, it is oriented towards one end of the oval. In summary, the polarized distribution of actin and tubulin is maintained in asymmetric *spa2* cells treated with pheromone but is lost in the large population of round *spa2* cells.

spa2 Mutants Do Not Mate Well with ste2-T326 Mutants, Which Are Also Defective in Shmoo Formation

Konopka et al. (1988) have constructed a mutation, *ste2-T326*, in the α-factor receptor gene that is impaired, but not completely defective, in its ability to induce shmoo formation (Konopka et al., 1988; Costigan, C., and M. Snyder, unpublished observations). We tested whether *spa2* mutants would mate well with *ste2-T326* mating partners using the low cell density conditions. As shown in Table II when the mating partner contains the *ste2-T326* mutation it mates with *spa2* cells at 17% the efficiency of when it is wild-type. Thus, the conjugation defect of *spa2* is enhanced when the mating partner contains the *ste2-T326* mutation.

DNA Sequence of the SPA2 Gene

In an effort to understand more about the function of the SPA2 protein, the DNA sequence of the *SPA2* gene was determined. The sequence of a 6.0-kb region containing *SPA2* is presented in Fig. 6. A single long open reading frame of 4,398 bp is present, capable of encoding a protein 1,466 amino acid residues in length. It is unlikely that an interven-

```
1    TCTAGAAGGAGACCTCATCGCCGATGTTACCTCAAAATTGAGTAGAATGAAATAATACAAAATTGGAAAAAACGCGAAACTTCAGTGCAGTAACATATCG
101  TTCCGACATTCTCTGAGAAGTGGTAAGATTCCACTGCCGGGGAGCTACGAGTGCTCTTGCAAGTTTTTAGACACTGCTATATCCTTCGACTACGTAACCC
201  CATTTTTTTATTTTTCTATATAAAAACATGCACTGTATACATATAATCACGTAAGTTCAAGTCGTGCTTAAAACGGGCACAGAAAACTAACTATGAGTTG
301  CCGTACCATACATAAACTAGGAGAAGGTAGCGCAGTTCTTTTTTTTTACCAAAGGTTTGCACAAAAAAGATGGTCTAACGTAAGTAAGTTATCAATAAAA
401  CTGTTAAAAGTAGTATAAGAATCTTGAGATAGGCTTATTATTATGACTTTTTATGGCGGAAAAGGAAGAAGAAATACTGCGCCGGGTGATGCGTGACGCG
501  TTTTTGGAAACGATGAGAATAAACTTTGAAGTATTTTGAGAATAATATTCTATTATCGAGTTCTTTCAGCAGAAAGCAACACATAGCTACGTATAGTTCG
601  GTAAGATAAATTTGGTCAGAAGCGTGTGAAAGACGCTGAGAAACCACGTGAGACGAAGATTCAAATCAAGGCGTGAGGAATAACGCAATACGAGCCACCG
701  AAACAGAATAAACAAAAGAAAAGAAAGAGTAAAC  ATG GGT ACG TCA AGC GAG GTT TCT CTC GCA CAT CAT AGA GAT ATC TTC
1                                   M   G   T   S   S   E   V   S   L   A   H   H   R   D   I   F

783  CAT TAC TAC GTC TCA CTG AAG ACT TTT TTC GAG GTG ACT GGC GAA AAT CGT GAC AGG TCA AAT TCG ACA CGA GCT
17   H   Y   Y   V   S   L   K   T   F   F   E   V   T   G   E   N   R   D   R   S   N   S   T   R   A

858  CAA AAG GCC AGA GCC AAG CTG TTG AAG CTA TCT TCT TCG CAA TTT TAC GAG CTG AGT ACA GAC GTG TCC GAT GAG
42   Q   K   A   R   A   K   L   L   K   L   S   S   S   Q   F   Y   E   L   S   T   D   V   S   D   E

933  CTG CAG AGG AGA ATC GGT GAA GAT GCT AAC CAA CCA GAT TAC CTT TTG CCG AAG GCA AAT TTC CAC ATG AAA AGG
67   L   Q   R   R   I   G   E   D   A   N   Q   P   D   Y   L   L   P   K   A   N   F   H   M   K   R

1008 AAC CAG GCT AGA CAG AAA CTG GCC AAT CTA TCA CAA ACT CGA TTT AAT GAT TTG TTG GAC GAT ATC CTT TTT GAG
92   N   Q   A   R   Q   K   L   A   N   L   S   Q   T   R   F   N   D   L   L   D   D   I   L   F   E

1083 ATC AAG AGA AGA GGG TTC GAC AAG GAT TTG GAT GCT CCA CGG CCC CCA TTA CCG CAG CCG ATG AAA CAA GAG GTC
117  I   K   R   R   G   F   D   K   D   L   D   A   P   R   P   P   L   P   Q   P   M   K   Q   E   V

1158 AGC AAA GAC AGC GAT GAT ACT GCA AGA ACA TCC ACA AAT TCT TCC TCT GTG ACT CAA GTA GCT CCA AAC GTC TCC
142  S   K   D   S   D   D   T   A   R   T   S   T   N   S   S   S   V   T   Q   V   A   P   N   V   S

1233 GTA CAA CCT TCT TTG GTC ATT CCT AAG ATG GCA TCT ATC GAT TGG TCT TCT GAG GAA GAA GAA GAG GAG CAA GTA
167  V   Q   P   S   L   V   I   P   K   M   A   S   I   D   W   S   S   E   E   E   E   E   E   Q   V

1308 AAG GAG AAG CCA AAT GAA CCG GAG GGA AAA CAA ACA AGC ATG GAT GAA AAG AAA GAG GCT AAA CCT GCT CTA AAC
192  K   E   K   P   N   E   P   E   G   K   Q   T   S   M   D   E   K   K   E   A   K   P   A   L   N

1383 CCC ATA GTT ACA GAT TCT GAT CTG CCT GAC TCC CAA GTG CTC GCT CGT GAT ATC ACA TCA ATG GCA AGG ACT CCA
217  P   I   V   T   D   S   D   L   P   D   S   Q   V   L   A   R   D   I   T   S   M   A   R   T   P

1458 ACA ACG ACG CAT AAA AAT TAC TGG GAC GTT AAT GAT TCT CCA ATT ATC AAG GTA GAT AAA GAT ATC GAT AAC GAA
242  T   T   T   H   K   N   Y   W   D   V   N   D   S   P   I   I   K   V   D   K   D   I   D   N   E

1533 AAG GGT CCC GAA CAG TTG AAG AGC CCT GAA GTA CAA CGG GCT GAG AAC AAT AAC CCT AAC TCA GAG ATG GAA GAC
267  K   G   P   E   Q   L   K   S   P   E   V   Q   R   A   E   N   N   N   P   N   S   E   M   E   D

1608 AAG GTT AAA GAA CTG ACT GAT TTA AAC AGC GAC TTA CAT TTG CAA ATT GAA GAT TTG AAT GCT AAG TTA GCA TCT
292  K   V   K   E   L   T   D   L   N   S   D   L   H   L   Q   I   E   D   L   N   A   K   L   A   S

1683 TTA ACC AGC GAG AAG GAA AAG GAG AAG AAG GAA GAG AAG GAG GAA AAA GAA AAG GAA AAG AAC TTA AAG ATT AAC
317  L   T   S   E   K   E   K   E   K   K   E   E   K   E   E   K   E   K   E   K   N   L   K   I   N

1758 TAC ACC ATT GAT GAA AGT TTT CAG AAA GAA TTG CTG TCA TTA AAC TCT CAA ATC GGT GAA TTA TCA ATT GAG AAT
342  Y   T   I   D   E   S   F   Q   K   E   L   L   S   L   N   S   Q   I   G   E   L   S   I   E   N

1833 GAA AAT TTG AAG CAG AAA ATT TCA GAA TTC GAA CTG CAT CAA AAA AAG AAT GAC AAC CAT AAT GAT TTG AAA ATC
367  E   N   L   K   Q   K   I   S   E   F   E   L   H   Q   K   K   N   D   N   H   N   D   L   K   I

1908 ACT GAC GGT TTT ATT AGC AAG TAC TCT TCT GCC GAT GGG CTC ATT CCA GCT CAA TAC ATC TTA AAC GCT AAC AAC
392  T   D   G   F   I   S   K   Y   S   S   A   D   G   L   I   P   A   Q   Y   I   L   N   A   N   N

1983 TTG ATA ATT CAA TTT ACT ACT AGG CTT TCC GCA GTA CCC ATA GGC GAC TCC ACG GCA ATT TCC CAT CAA ATT GGC
417  L   I   I   Q   F   T   T   R   L   S   A   V   P   I   G   D   S   T   A   I   S   H   Q   I   G

2058 GAA GAG TTA TTT CAA ATA TTA TCC CAG TTA TCG AAC CTA ATC TCC CAG CTA TTA CTA TCG GCC GAC CTA TTA CAG
442  E   E   L   F   Q   I   L   S   Q   L   S   N   L   I   S   Q   L   L   L   S   A   D   L   L   Q

2133 TAC AAA GAT CAG GTC ATT TTA CTG AAG GCA TCA TTA TCG CAT GCG ATC ACA TCG ATA AGA TAT TTC TCT GTT TAC
467  Y   K   D   Q   V   I   L   L   K   A   S   L   S   H   A   I   T   S   I   R   Y   F   S   V   Y

2208 GGT CCC GTA TTA ATT CCG AAA ATA ACT GTG CAA GCT GCT GTT TCA GAG GTT TGT TTT GCC ATG TGT AAT CTA ATT
492  G   P   V   L   I   P   K   I   T   V   Q   A   A   V   S   E   V   C   F   A   M   C   N   L   I

2283 GAT TCA GCG AAA ATA AAA TCC GAT TCA AAT GGT GAG AGC ACC ACC TCT AAT GAA GGT AAC CGA CAG GTA TTA GAA
517  D   S   A   K   I   K   S   D   S   N   G   E   S   T   T   S   N   E   G   N   R   Q   V   L   E

2358 TAT TCT TCA CCA ACT GCT ACC ACC CCA ATG ACG CCA ACT TTC CCC TCG ACT TCT GGA ATA AAT ATG AAG AAG GGG
542  Y   S   S   P   T   A   T   T   P   M   T   P   T   F   P   S   T   S   G   I   N   M   K   K   G

2433 TTT ATA AAC CCA AGA AAA CCA GCA TCT TTC TTG AAT GAT GTG GAG GAA GAA GAA TCT CCA GTC AAG CCA TTG AAA
567  F   I   N   P   R   K   P   A   S   F   L   N   D   V   E   E   E   E   S   P   V   K   P   L   K

2508 ATT ACA CAA AAG GCA ATT AAC AGT CCG ATC ATA AGA CCG TCA TCG TCT AAT GGA GTT CCA ACA ACC TCA AGA AAA
592  I   T   Q   K   A   I   N   S   P   I   I   R   P   S   S   S   N   G   V   P   T   T   S   R   K

2583 CCT TCA GGA ACG GGG CTA TTT AGT TTA ATG ATT GAT TCA TCA ATT GCT AAG AAT AGC TCC CAT AAA GAG GAT AAT
617  P   S   G   T   G   L   F   S   L   M   I   D   S   S   I   A   K   N   S   S   H   K   E   D   N

2658 GAT AAA TAT GTC TCG CCC ATA AAG GCA GTA ACA TCG GCC TCC AAT TCT GCA AGT AGC AAT ATT TCC GAA ATT CCT
642  D   K   Y   V   S   P   I   K   A   V   T   S   A   S   N   S   A   S   S   N   I   S   E   I   P

2733 AAA CTA ACA CTA CCT CCA CAA GCC AAA ATC GGT ACT GTT ATT CCA CCG TCA GAG AAT CAA GTT CCC AAT ATT AAA
667  K   L   T   L   P   P   Q   A   K   I   G   T   V   I   P   P   S   E   N   Q   V   P   N   I   K

2808 ATC GAG AAT ACA GAA GAG GAT AAT AAA AGG AGT GAC ATA ACA AAT GAA ATC TCT GTT AAA CCA ACT TCT AGC ATT
692  I   E   N   T   E   E   D   N   K   R   S   D   I   T   N   E   I   S   V   K   P   T   S   S   I

2883 GCT GAT AAA CTG AAA CAA TTT GAG CAA AGT TCC GAA AAG AAA TCA TCA CCA AAG GAA AAT CCT ATA GCA AAA GAA
717  A   D   K   L   K   Q   F   E   Q   S   S   E   K   K   S   S   P   K   E   N   P   I   A   K   E
```

Figure 6. DNA sequence of the *SPA2* locus. The translation of the *SPA2* long open reading frame is depicted beneath the DNA sequence. Numbers adjacent to the nucleotide refer to the nucleotide position; numbers in italics refer to the amino acid residue position downstream of the predicted initiator methionine. The underlined nucleotides represent the termination codon of an open reading frame from a gene that is convergently transcribed towards *SPA2*. These sequence data are available from EMBL/GenBank/DDBJ under accession number X53731.

```
2958 GAA ATG GAT TCA AAA CCA AAA CTA TCC AAT AAA TTT ATC ACT TCA ATG AAT GAT GTG TCC ACA GAT GAT TCA AGC
742  E   M   D   S   K   P   K   L   S   N   K   F   I   T   S   M   N   D   V   S   T   D   D   S   S

3033 TCT GAT GGT AAC GAA AAT GAC GAT GCA GAC GAT GAT GAT GAT TTT ACC TAT ATG GCA TTG AAA CAA ACA ATG AAG
767  S   D   G   N   E   N   D   D   A   D   D   D   D   D   F   T   Y   M   A   L   K   Q   T   M   K

3108 AGA GAA GGT TCA AAA ATT GAA AAA AAT AAT GAC AGC AAA CTA CCT GCA AAT ATA GTG GAA CTT GAT TTA CAT GAG
792  R   E   G   S   K   I   E   K   N   N   D   S   K   L   P   A   N   I   V   E   L   D   L   H   E

3183 TCA CCG GAG TCC GTG AAG ATT GAA TCT CCT GAA TCG ATA AAG GAA ATC ACG TCA TCT GAA ATG TCT TCA GAA ATG
817  S   P   E   S   V   K   I   E   S   P   E   S   I   K   E   I   T   S   S   E   M   S   S   E   M

3258 CCA AGT AGT TCG CTG CCT AAG AGA TTA GTA GAG GAT GTT GAG CCT TCA GAA ATG CCA GAG AAG GGC GCA TCT GTA
842  P   S   S   S   L   P   K   R   L   V   E   D   V   E   P   S   E   M   P   E   K   G   A   S   V

3333 GAA TCA GTC AGG AAG AAA AAT TTT CAA GAA CCA CTT GGT AAT GTC GAA TCT CCG GAT ATG ACG CAG AAG GTC AAG
867  E   S   V   R   K   K   N   F   Q   E   P   L   G   N   V   E   S   P   D   M   T   Q   K   V   K

3408 TCT TTG GGT ATG ACA GGA AAG GCT GTA GGC CCA GAA TCA GAT AGT AGG GTC GAA TCT CCG GGC ATG ACA GGA CAG
892  S   L   G   M   T   G   K   A   V   G   P   E   S   D   S   R   V   E   S   P   G   M   T   G   Q

3483 ATT AAA TCT TTG AAT ATG GCA GGA AAA GTT GTA GGC CCA GAA GCA GAT AGT AGG GTC GAA TCT CCG GGC ATG AAA
917  I   K   S   L   N   M   A   G   K   V   V   G   P   E   A   D   S   R   V   E   S   P   G   M   K

3558 GAG CAG ATT AAG TCT TTG GGT ATG ACA GGA AAA ATT ACA GCT CAA GAA TCA ATC AAG TCC CCG GAA GCG GCT AGG
942  E   Q   I   K   S   L   G   M   T   G   K   I   T   A   Q   E   S   I   K   S   P   E   A   A   R

3633 AAG TTG GCG TCA TCA GGA GAA GTT GAC AAA ATT GAA TCT CCA AGA ATG GTA AGG GAA AGC GAG TCC TTG GAG GCA
967  K   L   A   S   S   G   E   V   D   K   I   E   S   P   R   M   V   R   E   S   E   S   L   E   A

3708 GTA GGC AAT ACT ATC CCC TCA AAC ATG ACA GTG AAA ATG GAA TCC CCA AAT TTA AAG GGA AAT ACT GTG TCT GAA
992  V   G   N   T   I   P   S   N   M   T   V   K   M   E   S   P   N   L   K   G   N   T   V   S   E

3783 CCT CAA GAA ATA AGG AGA GAC ATT GCC TCC TCA GAG CCG ATA GAG AAT GTT GAC CCC CCA AAA GTA CTA AAA AAG
1017 P   Q   E   I   R   R   D   I   A   S   S   E   P   I   E   N   V   D   P   P   K   V   L   K   K

3858 ATT GTC TTT CCA AAG GCT GTT AAT AGA ACT GGA TCA CCA AAA TCA GTC GAA AAG ACT CCA TCT TCA GCT ACA CTG
1042 I   V   F   P   K   A   V   N   R   T   G   S   P   K   S   V   E   K   T   P   S   S   A   T   L

3933 AAA AAG AGC GGG CTC CCA GAA CCG AAT AGC CAA ATT GTT TCT CCT GAA TTG GCA AAA AAT TCA CCT CTA GCA CCG
1067 K   K   S   G   L   P   E   P   N   S   Q   I   V   S   P   E   L   A   K   N   S   P   L   A   P

4008 ATA AAG AAA AAT GTC GAG TTA CGA GAA ACT AAT AAA CCA CAT ACT GAG ACT ATC ACT TCT GTG GAA CCA ACA AAC
1092 I   K   K   N   V   E   L   R   E   T   N   K   P   H   T   E   T   I   T   S   V   E   P   T   N

4083 AAG GAT GCC AAT ACT TCT TGG AGA GAC GCC GAC TTA AAC CGT ACG ATC AAA CGA GAG GAG GAG GAC GAA GAT TTT
1117 K   D   A   N   T   S   W   R   D   A   D   L   N   R   T   I   K   R   E   E   E   D   E   D   F

4158 GAT AGA GTG AAC CAC AAT ATC CAG ATC ACT GGT GCA TAT ACG AAA ACT GGA AAA ATT GAT TAT CAT AAA ATA CCT
1142 D   R   V   N   H   N   I   Q   I   T   G   A   Y   T   K   T   G   K   I   D   Y   H   K   I   P

4233 GTT GAT CGT AAA GCA AAA AGC GAA GCA GAA GTG CAT ACT TCC GAG GAA GAT ATT GAT GAA TCA AAT AAT GTT AAT
1167 V   D   R   K   A   K   S   E   A   E   V   H   T   S   E   E   D   I   D   E   S   N   N   V   N

4308 GGA AAA AGA GCT GAT GCC CAA ATA CAC ATC ACT GAA AGA AAG CAT GCT TTC GTA AAT CCA ACT GAA AAT TCA CAG
1192 G   K   R   A   D   A   Q   I   H   I   T   E   R   K   H   A   F   V   N   P   T   E   N   S   Q

4383 GTA AAA AAG ACG AGC CAC TCA CCA TTT TTA AAC AGT AAA CCG GTT CAA TAC GAG AAC TCA GAG TCG AAC GGC GGC
1217 V   K   K   T   S   H   S   P   F   L   N   S   K   P   V   Q   Y   E   N   S   E   S   N   G   G

4458 ATT AAC AAC CAC ATA AAG ATA AAA AAT ACT GGA GAA ACT ACG GCA CAT GAC GAG AAA CAT TAT AGT GAT GAT GAT
1242 I   N   N   H   I   K   I   K   N   T   G   E   T   T   A   H   D   E   K   H   Y   S   D   D   D

4533 GAT TCT AGC TAT CAA TTT GTT CCC ATG AAA CAT GAA GAA CAA GAA CAA GAA CAA AAC AGA AGT GAG GAA GAG GAA
1267 D   S   S   Y   Q   F   V   P   M   K   H   E   E   Q   E   Q   E   Q   N   R   S   E   E   E   E

4608 AGT GAA GAT GAC GAT GAA GAG GAA GAA GAC AGT GAT TTT GAT GTG GAT ACA TTT GAC ATT GAA AAT CCG GAT AAT
1292 S   E   D   D   D   E   E   E   E   D   S   D   F   D   V   D   T   F   D   I   E   N   P   D   N

4683 ACA CTA TCA GAG TTA CTA TTG TAT TTA GAA CAT CAA ACA ATG GAC GTC ATA TCC ACG ATT CAA TCG CTT TTG ACA
1317 T   L   S   E   L   L   L   Y   L   E   H   Q   T   M   D   V   I   S   T   I   Q   S   L   L   T

4758 TCG ATC AAG AAA CCA CAG GTG ACG AAG GGT AAT TTG AGG GGA GAA TCG AAT GCA ATC AAC CAA GTC ATA GGT CAA
1342 S   I   K   K   P   Q   V   T   K   G   N   L   R   G   E   S   N   A   I   N   Q   V   I   G   Q

4833 ATG GTG GAC GCT ACT AGC ATA TCA ATG GAG CAA AGC AGA AAT GCC AAT TTG AAG AAA CAC GGT GAT TGG GTG GTG
1367 M   V   D   A   T   S   I   S   M   E   Q   S   R   N   A   N   L   K   K   H   G   D   W   V   V

4908 CAA AGT CTA AGA GAC TGT TCG CGT AGA ATG ACA ATT TTG TGC CAA TTA ACT GGC GAT GGA ATA CTA GCG AAG GAA
1392 Q   S   L   R   D   C   S   R   R   M   T   I   L   C   Q   L   T   G   D   G   I   L   A   K   E

4983 AAG AGC GAT CAA GAT TAT GCT GAC AAA AAC TTC AAA CAG CGG TTG GCA GGG ATT GCG TTT GAT GTT GCC AAA TGT
1417 K   S   D   Q   D   Y   A   D   K   N   F   K   Q   R   L   A   G   I   A   F   D   V   A   K   C

5058 ACA AAG GAG CTG GTA AAA ACT GTA GAA GAG GCA AGT TTG AAG GAC GAA ATA AAT TAT TTG AAT TCG AAG TTG AAG
1442 T   K   E   L   V   K   T   V   E   E   A   S   L   K   D   E   I   N   Y   L   N   S   K   L   K

5133 TAA AGTTAGTAGTATCTAGAGGAGAAAGAAAAGGAAGACAAAGACAATCAATAGAATGTATTATGTATGACATATAATAATAATAATTATAATAATAA
1467 Trm
5230 TAATAATAGTAGTAGCAGTAATAATAATATTATTATAGTATATTAAAACAACAAAAAATTAGTAAAAATACTATAAATGTTTGAATATGAAGATATATA
5330 TGTAGGAAGAATTTTTATTGAATATAGAAATTTAAAGAAATATTATTAAAAACCGGAAAATGAAAAAGAAGAGTTAAAAAAAAAAAAAAACGGAACTAGT
5430 AAAAGATGTGAAAAAAAGAAGAGAAAAGTAGAACGAGAACACCCACTATCCTTGGGTATTATTATAAGTTGCAATACCATCATCCAGTATGCCCAGATT
5530 AAACCATTCATGGTCCAGAGCGTCCTTTGCGGTAATCCTTTTTGTTGGGTCGAACTCAAACATTTTCCTGAGTAGATCGATGAACCAGTACCAAAACAA
5630 GAAAGTTTCCTTATCGAGTTCATCAGTAGTTGAGGAAGAAGAGGAATGTGTTTGTCTTTTCCATGCCAATTTCGAATTTATCAAAGACCAGTTTTTCTC
5730 CGGCGGTAGATTCCAATTGATGCTTAAGCTATCGCCGTAATCCTGTTTCAAGACCTTTGAGATGTAAATATCTAAGCGATCACATGACTGCAAGACCCT
5830 TTTCATTGACTTTTCGGTGGTTATGGTATCTCCGCGTTTATTTTTTTCAGGCCATTGTAAGCTTAAAGTTTTTCTGTCGAAATGCTTTATCACCGTTGA
5930 ATTTAGGTCTGATGGAGAGTTGCCCAATTTATGTTTAGGGTTCCATTGATTCGTTGCATCATAGCCATATGTTCTAGA
```

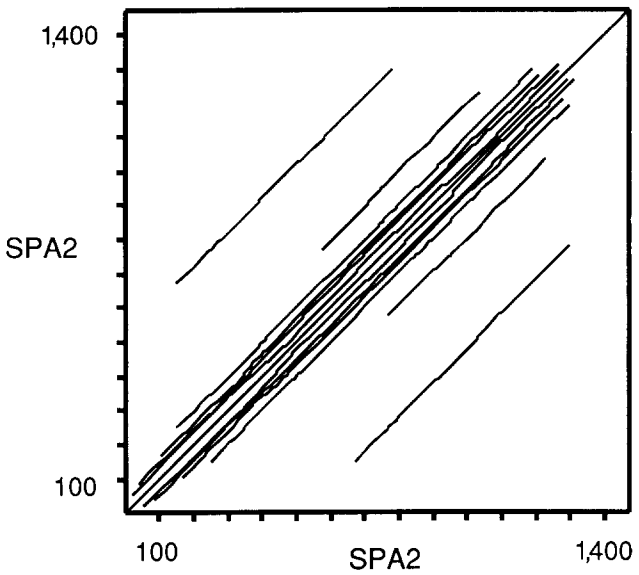

Figure 7. Internal sequence similarities within the predicted protein sequence of SPA2. Using the pLFASTA programs of Pearson and Lipman (1988), the predicted SPA2 protein sequence was compared with itself. Diagonal lines indicate regions of sequence similarities.

ing sequence lies within the *SPA2* protein coding region, since this sequence lacks the TACTAAC sequence found close to the 3′ end of all yeast introns (Teem et al., 1984). 339 bp downstream of the *SPA2* open reading frame lies another long open reading frame that is convergently transcribed towards *SPA2*. This open reading frame encodes a protein kinase homologue and will be described elsewhere.

As deduced from the DNA sequence, the SPA2 protein is very hydrophilic; it contains 16.9% acidic (glu and asp) and 12.9% basic (lys and arg) residues. The DNA sequence also predicts a large protein of 160 kD in molecular mass, in reasonable agreement with the 180-kD estimate from immunoblot analysis (Snyder, 1989). The slight discrepancy between these figures may be due to several possibilities including posttranslational modifications of the protein in vivo. In this respect, we note that the SPA2 protein is rich in serine and threonine residues (17.8%), which are potential sites of phosphorylation.

Repeat #	aa 816
	ES
1	PESVK-IES
2	PESIKEITS
3	SEMSSEMPS[16 aa]
4	PEKGASVES[6 aa]
5	QEPLGNVES
6	PDMTQKVKS
7	LGMTGKAVG
8	PESDSRVES
9	PGMTGQIKS
10	LNMAGKVVG
11	PEADSRVES
12	PGMKEQIKS
13	LGMTGKI--
14	-TAQESIKS
15	PEAARKLAS
16	SGEVDKIES
17	PRMVRESES
18	LFAVGNTIP
19	SNMTVKMES
20	PNLKGNTVS[20 aa]
21	PKVLKKIVF
22	PKAVNRTGS
23	PKSVEKTPS[9 aa]
24	PEPNSQIVS
25	PELAKNS
	aa 1087
Consensus	PEMVGKOES
Frequency	16 11 9 6 7 9 20 9 20
Alternative residues	LGSTKR V 4 5 4 5 4 3 5
Hydrophobic	* * *

Figure 8. The imperfect nine amino acid repeat of the SPA2 protein. This sequence is interrupted at the four indicated positions by insertions of 6–20 amino acids. For the consensus sequence, 0 = hydrophobic. Note that residues 1, 3 and/or 4, and 7 are typically hydrophobic. Higher order similarities of the repeats are present; for example, the sequence of repeats 6–8 is very similar to that of 9–11, and that of 6–7 is very similar to that of 9–10 and 12–13.

The SPA2 Protein Sequence Contains a Number of Internal Repeats

When segments of the predicted SPA2 protein sequence were compared with each other, a variety of internal repetitive elements were revealed. Portions of the first half of the protein sequence show low-level (20%) sequence identity with the second half of the molecule (Fig. 7). Of particular interest is a nine amino acid sequence, which is imperfectly repeated 25 times (residues 816–1,087; Fig. 8). This short repeat accounts for the closely spaced lines just off the main diagonal in Fig. 7. Hydrophobic residues within this nine amino acid repeat are spaced at positions 1 (which is usually a proline), 3 and/or 4, and 7. The most conserved part of the repeat is a four amino acid stretch consisting of a hydrophobic residue followed by X-Ser-Pro (X = any amino acid). (Note in Fig. 8 this sequence starts in one repeat and extends into the next one.) In many cases, these nonapeptide units can be arranged into higher order 18- and 27-amino acid repeats. (Examples are provided in the legend to Fig. 8.) Possible structures for this region are described in the discussion.

The SPA2 Sequence Contains Low-level Sequence Similarity to Coiled-coil Proteins

The predicted amino acid sequence of the *SPA2* gene was compared to those in the NBRF-PIR data base using the FASTA programs (Pearson and Lipman, 1988); this comparison revealed that portions of the *SPA2* gene product have significant amino acid sequence similarity to a variety of proteins that form coiled-coil structures. The highest matches were between a 200 residue stretch near the amino terminus (residues 281–488) and type I keratins and cytokeratins (Table IV). For example, this sequence is 24% identical and 35–74% similar to the 59-kD keratin protein of mouse (Fig. 9). Segments within this region are predicted to form an α-helix, and many portions exhibit the characteristic heptad spacing of hydrophobic residues that is found in coiled-coil proteins; many of these hydrophobic residues are leucines (Fig. 9; see Discussion).

A 1,106 amino acid stretch of the SPA2 protein (residues 139–1,223) shows a low-level sequence similarity to the myosin heavy chain of chicken and nematodes, and to other coiled-coil proteins. Some of the homologous region corresponds to the potential coiled-coil portion at the amino terminus described above, but much of it lies closer to the carboxy terminus, where the ability of the SPA2 protein to form a coiled-coil structure is less clear (see Discussion).

Short stretches of acidic amino acids are also present in

Table IV. Amino Acid Similarity between the SPA2 Protein and Proteins that Form Filaments

Protein	Residues	Residues SPA2	Length	Identity	Similarity	FASTA score	Reference
				%	%		
Keratin, 47 kD Type I, mouse	69–275	281–488	212	22 (6)	39–74	109	Knapp et al. (1986)
Keratin, 59 kD Type I, mouse	244–417	281–460	182	24 (3)	35–74	97	Krieg et al. (1985)
Keratin, 50 kD Type I, human	213–418	281–488	212	17 (6)	34–73	90	Marchuk et al. (1985)
Cytokeratin 19, bovine	153–382	258–488	236	18 (8)	34–74	105	Bader et al. (1986)
Myosin Heavy Chain, chicken	859–1,939	139–1,223	1106	14 (23)	30–70	143	Molina et al. (1987)
Myosin Heavy Chain, nematode	910–1,685	680–1,454	791	12 (15)	30–70	115	Karn et al. (1983)
Neurofilament, triplet H, human	742–1,020	523–806	291	20 (7)	32–74	116	Lees et al. (1988)

Amino acid similarity between the SPA2 protein and proteins that form coiled-coil structures. The numbers in brackets under % identity indicate the number of gaps used to maximize the alignment. The % similarity varies, depending upon the criteria used. The first number indicates the most stringent criteria (identities plus E = D, K = R, Q = N, I = L = A = V = M, F = Y); the second number indicates the more liberal matches used by the FASTA program. Additional matches were found to other keratin sequences; the sequences listed encompass the range of similarities. The portion of the neurofilament protein that is homologous to the SPA2 protein is predicted to form an α-helix, but may not form a coiled-coil structure. This region of the SPA2 protein is also predicted to form an α-helix.

the putative SPA2 protein. The location of these acidic regions and the different features concerning the SPA2 protein sequence are summarized in Fig. 10.

Discussion

The Role of SPA2 in Cellular Morphogenesis and Mating

Analysis of a large deletion of the *SPA2* gene revealed that *SPA2* is important for efficient mating and shmoo formation. If the defect of *spa2* mutant cells is primarily in the synthesis of morphological projections, then we conclude that shmoo formation is an important step in the mating process. Since *spa2* mutants appear marginally rounder than wild-type cells (Snyder, 1989), the inability to form appropriate shmoos is consistent with an overall morphological defect and with the hypothesis that SPA2 plays a role as a cytoskeletal component (see below).

The major defect of *spa2* mutants occurs principally when they are mated to other *spa2* mutants; the mating efficiency of *spa2* mutants is only 1–2% that of wild-type at high cell densities, and <0.1% at low cell densities. When mated with wild-type strains at high cell densities, *spa2* mutants conjugate at reasonable levels, 73–23% that of wild-type cells. Consistent with these results, Konopka et al. (1988) have found that at high cell densities, *ste2-T326* mutants mate with wild-type cells at 60% the efficiency of wild-type cell matings. Thus, we suggest that shmoo formation by one mating partner is often sufficient to make the appropriate contact with the other partner, especially at high cell densities. As might be expected for mutants defective in shmoo formation, at a lower cell density when cells are spaced further apart, the relative mating efficiency becomes substantially reduced

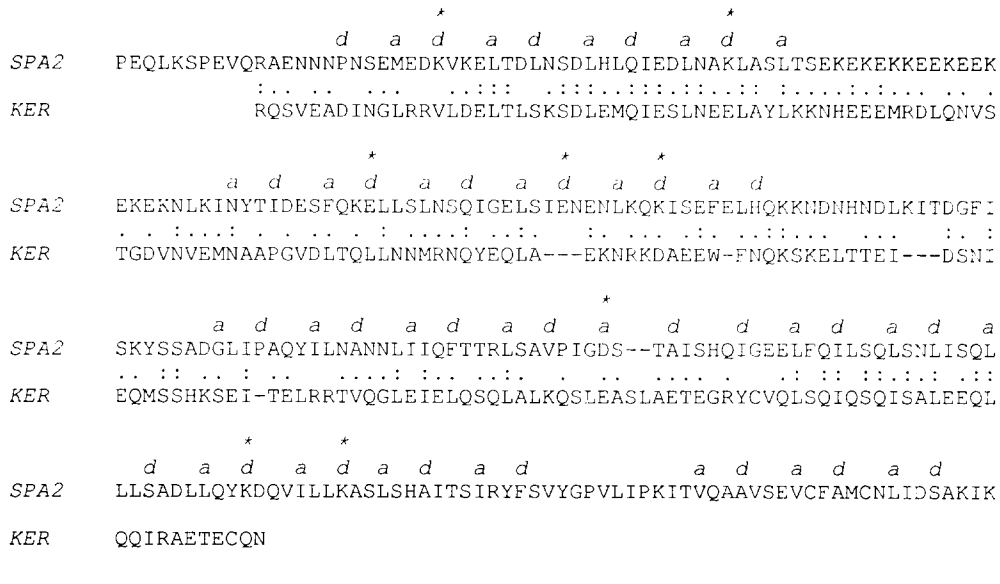

Figure 9. Low-level sequence similarity between the SPA2 protein and proteins that form coiled-coil structures. For exemplary purposes, the 59-kD Type I keratin of mouse is aligned with SPA2. The SPA2 sequence begins at amino acid 270 and extends to residue 523. The keratin sequence begins at amino acid 243 and extends to residue 427. Identical residues are indicated by a colon. Similar residues are noted by a period. Overall, the sequence is 24% identical. The number of identical and similar residues depends on the criteria used; this value ranges from 35% for the most stringent possibilities, to 74% similar for more liberal interpretations using the FASTA alignments which are shown. Matches between SPA2 and other proteins that form coiled-coil structures are listed in Table IV. Five regions within this sequence are predicted to be capable of forming coiled-coil structures; the last is rather short. For these regions the heptad periodicity (*abcdefg*) is noted by *a* and *d* symbols above the sequence; these usually correspond to hydrophobic residues. A polar residue at these positions which would destabilize associations between subunits is indicated by an *. The regions between the heptad regions differ in size from those of intermediate filament proteins.

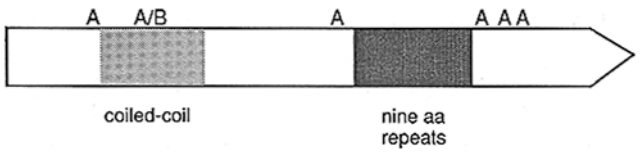

Figure 10. Predicted features of the SPA2 protein. Indicated are the region capable of forming coiled-coil structures and the nine amino acids repeats. The *A* indicates acidic regions where greater than six out of ten residues are acidic. These correspond to the following positions (from left to right) 180–189; 771–780; 1135–1142; 1258–1267; and 1288–1312. *A/B* denotes a highly charged region at residues 320–336 that contains both basic and acidic residues.

for the unilateral (*spa2*::wild type) and particularly the bilateral (*spa2*::*spa2*) matings.

spa2 mutants also display an enhanced conjugation defect when mated with *ste2-T326* cells (sixfold as compared to matings between *spa2* cells and wild-type cells). This observation is consistent with the expectation that conjugation defects are most severe when both partners are defective in shmoo formation. The defect appears much more severe when both partners contain a *spa2* mutation than when one carries a *spa2* mutation and the other contains *ste2-T326*. This difference may be due to the different strain backgrounds, the possibility that *spa2* is defective in other aspects of mating besides shmoo formation (see below), or that the shmoo defect is more severe in *spa2* mutants than *ste2-T326* mutants (Costigan, C., and M. Snyder, unpublished observations).

It is possible that *spa2* mutants are impaired in other aspects of the mating process in addition to shmoo formation and that such defects contribute to the decreased mating efficiency. For example, nuclear fusion is impaired in *spa2* matings as evidenced by an increase in the number of cytoductants; perhaps this reflects an inability of the nuclei to orient properly during the mating process. This nuclear fusion defect is not enough to account for the overall 50–100-fold mating defect observed under similar conditions. It is possible that the SPA2 protein also plays a role in cytoskeletal reorganization during or after conjugation. If these defects lead to cell death, they would not be detected by the cytoductant assays.

spa2 deletion mutants still form buds well, but have a severe defect in the formation of shmoo projections. Thus, polarized growth in shmoos appears more dependent on the SPA2 protein than polarized growth in mitotic cells. Perhaps a protein or set of proteins with a function related to SPA2 is present in vegetative cells, but is absent or reduced in mating cells.

The different *spa2* alleles have slightly different phenotypes. The insertion alleles originally constructed, *spa2-8* and particularly *spa2-7*, have the strongest defects in budding patterns (Snyder, 1989). Although mating efficiencies of strains with these alleles were not quantitated, no obvious defect was noticed during a number of crosses. When *spa2-7* and *spa2-8 MATa* cells were treated with α-factor, intermediate levels of shmoo formation were observed relative to wild-type and *spa2-Δ2* cells. Thus, we suspect that the deletion alleles described here confer the strongest mating defect. Cells containing the *spa2-Δ2* and *spa2-Δ3* alleles have weaker budding pattern defects than those containing the insertion alleles; hence, the insertion alleles may produce products that interfere with normal cellular functions (see Snyder, 1989).

SPA2, Actin, and Tubulin Polarity in Pheromone-treated Cells

The cytological staining experiments indicate that both actin and tubulin have polarized distributions in cells treated with mating pheromone (Hasek et al., 1987; Figs. 4 and 5). The localization of both these cytoskeletal components is consistent with expectations based on their distribution in mitotic cells. In unbudded cells, actin spots concentrate at the site where bud formation is expected to begin; in budded cells, actin spots are found near the bud surface. Actin cables and a few spots are present in the mother cell. In shmoos, actin spots concentrate near the surface of the projection, preferentially in the tip region. Hence, both in mitotic cells and in pheromone-induced cells, actin spots localize to regions of polarized growth near the cell surface. The SPA2 protein is also in these regions, but is not present in large spots, and is much more distinctly localized to the bud tips in budded cells and the growing projections in shmoos.

As recently noted by Baba et al. (1989) and Hasek et al. (1987), the location of the SPB is also polarized in pheromone-treated cells; the SPB lies on the side of the nucleus nearest the projection tip. The immunofluorescence experiments presented above indicate that one or more long tubulin bundles extend back to the main cell body. Occasionally, a short tubulin bundle intersects the SPA2 patch at the shmoo tip. However, not all pheromone-treated cells contain a bundle that extends to the projection tip. Therefore, either only a fraction of the cells have this feature or the fixation or staining conditions failed to preserve or detect bundles that may have been present initially. Interestingly, *cdc28* mutants, which arrest with a morphology similar to that of pheromone-treated cells, always contain a long extranuclear microtubule bundle that intersects the SPA2 staining region (B. Page and M. Snyder, unpublished observations).

This intersection of the tips of microtubules with the SPA2 staining region is consistent with that observed in vegetatively growing cells, whereby long extranuclear microtubule bundles are observed to extend into the bud (Byers, 1981; Snyder, 1989). Indeed, double immunofluorescence experiments using both antitubulin and anti-SPA2 antibodies reveal that most budded and many unbudded cells contain a long microtubule that intersects the SPA2 staining region (Snyder, M., unpublished observations). Since the SPA2 protein and gene was originally identified with anticentrosomal antibodies, these locations are consistent with the hypothesis that the SPA2 protein directly or indirectly interacts with the ends of microtubules (Snyder, 1989).

If the SPA2 protein is a cytoskeletal component, then its presence might affect the localization of actin and tubulin. *spa2* mutant cells that exhibit asymmetric morphology upon exposure to mating pheromone (oval cells and shmoo-like cells) usually contain a polarized localization of actin and tubulin indicating that the SPA2 protein is not absolutely essential for their distribution. However, since cell shape is completely disrupted in a large fraction of the cells (i.e., 41% are round), the SPA2 protein may contribute to cell polarity, and this might be achieved through affecting the dis-

tribution of actin and/or tubulin. Studies to examine the localization of the SPA2 protein in mutants defective in actin or tubulin may determine whether these proteins control the distribution of the SPA2 protein.

The SPA2 Protein Is Related to Coiled-coil Proteins

The predicted SPA2 protein is large, contains a number of internal repeats, and also contains low sequence similarity to that of many coiled-coil proteins. In a coiled-coil protein two α-helices interact at a hydrophobic interface to form a dimer. To generate the interface, hydrophobic residues are spaced at every first and fourth residue in a heptad repeat (positions *a* and *d* in Fig. 9). Portions of the amino terminus of the SPA2 protein are capable of forming an α-helix and also contain the appropriate spacings of hydrophobic residues, consistent with a coiled-coil structure. Many of the hydrophobic residues are leucines, characteristic of the "leucine zipper" class of coiled-coil interactions (Landschulz et al., 1988). Perhaps the SPA2 protein is oligomeric and/or forms a filament. For the carboxy terminal portion which contains the internal nine amino acid repeats, the ability to form a coiled-coil structure is less clear.

The SPA2 Internal Repeats

Particularly striking within the predicted SPA2 protein is the presence of a nine amino acid sequence imperfectly repeated 25 times. The most conserved portion of this repeat is the sequence: hydrophobic residue-X-Ser-Pro. This region might assume one of a number of possible structures. This sequence contains a proline, which is typically a "helix breaker". However, there are examples of a proline residue in an α-helix; their presence causes the helix to bend (for example see Katti et al., 1990). Using CPK models based on an 11 amino acid sequence containing one of the SPA2 repeats, LGNVESPDMTQ (portions of repeats 5 and 6), we were able to fold this sequence into an α-helix. We propose that the serine preceding the proline might help stabilize an α-helix by hydrogen bonding with the free amide oxygen two residues upstream. Other proteins contain S-P dipeptides (Noble et al., 1989); therefore, this proposed stabilization may be a general phenomenon.

If this region is in an α-helix, the presence of three positions containing hydrophobic residues in the nine amino acid repeat region could potentially provide a hydrophobic face for protein–protein interactions. However, the pitch is too steep to accommodate the traditional coiled-coil structure described above. Thus, it appears likely that it either remains unassociated with other subunits, or is arranged in a novel configuration with one or more subunits. Alternatively, it is possible that this region is not in an α-helix, but is in some other unique conformation. Further analysis will be required to determine the structure of this region.

The motif Polar residue-Ser-Pro which occurs in most of the repeats is also interesting because it is similar to the $p34^{cdc2}$ phosphorylation recognition sequence Polar-Ser/Thr-Pro-X-Basic described by others (Shenoy et al., 1989). Perhaps the SPA2 protein is phosphorylated by a member of the CDC2/CDC28 protein kinase family, such as the FUS3 protein, which has recently been shown to be important for early steps in the mating process (Elion et al., 1990).

Conclusion

Shmoo formation is a type of morphological differentiation that can be readily analyzed using a simple eukaryote. Further analysis of *SPA2* and other genes that affect pheromone-induced morphogenesis in yeast may provide a model system for understanding the mechanisms that govern cellular morphogenesis in larger eukaryotes.

We thank C. Costigan, R. Fox, C. Jackson, C. Mann, and B. Page for useful suggestions; and C. Copeland, C. Costigan, B. Grimwade, T. Menees, R. Padmanabha, B. Rockmill, and S. Roeder for critical comments on the manuscript.

This work was supported by National Institutes of Health grant GM36494 and used equipment purchased with funds from the Pew scholar's program.

Received for publication 6 April 1990 and in revised form 15 June 1990.

References

Adams, A. E. M., and J. R. Pringle. 1984. Relationship of actin and tubulin distribution to bud growth in wild-type and morphogenetic- mutant *Saccharomyces cerevisiae*. *J. Cell Biol.* 98:934–945.

Adams, A. E., D. Botstein, and D. G. Drubin. 1989. A yeast actin-binding protein is encoded by SAC6, a gene found by suppression of an actin mutation. *Science (Wash. DC).* 243:231–233.

Baba, M., N. Baba, Y. Ohsumi, K. Kanaya, and M. Osumi. 1989. Three-dimensional analysis of morphogenesis induced by mating pheromone α factor in *Saccharomyces cerevisiae*. *J. Cell Sci.* 94:207–216.

Bader, B. L., T. M. Magin, M. Hatzfeld, and W. W. Franke. 1986. Amino acid sequence and gene organization of cytokeratin no. 19, an exceptional tail-less intermediate filament protein. *EMBO (Eur. Mol. Biol. Organ.) J.* 5:1865–1875.

Byers, B. 1981. Cytology of the yeast life cycle. *In* The Molecular Biology of the Yeast Saccharomyces: Life Cycle and Inheritance. J. N. Strathern, E. W. Jones, and J. R. Broach, editors. Cold Spring Harbor Laboratory, Cold Spring Harbor, NY. 59–96.

Conde, J., and G. R. Fink. 1976. A mutant of Saccharomyces cerevisiae defective for nuclear fusion. *Proc. Natl. Acad. Sci. USA.* 73:3651–3655.

Cross, F., L. H. Hartwell, C. Jackson, and J. B. Konopka. 1988. Conjugation in *Saccharomyces cerevisiae*. *Annu. Rev. Cell Biol.* 4:429–457.

Davis, R. W., D. Botstein, and J. R. Roth. 1980. Advanced Bacterial Genetics. Cold Spring Harbor Laboratory, Cold Spring Harbor, NY. 254 pp.

Drubin, D. G. 1990. Actin and actin-binding proteins in yeast. *Cell Motil. Cytoskeleton.* 15:7–11.

Drubin, D. G., K. G. Miller, and D. Botstein. 1988. Yeast actin-binding proteins: evidence for a role in morphogenesis. *J. Cell Biol.* 107:2551–2561.

Elion, E. A., P. L. Grisafi, and G. R. Fink. 1990. *FUS3* encodes a cdc2+/CDC28-related kinase required for the transition from mitosis into conjugation. *Cell.* 60:649–664.

Feinberg, A. P., and B. Vogelstein. 1983. A technique for radiolabeling DNA restriction endonuclease fragments to high specific activity. *Anal. Biochem.* 132:6–13.

Haarer, B., and J. R. Pringle. 1987. Immunofluorescence localization of the Saccharomyces cerevisiae *CDC12* gene product to the vicinity of the 10-nm filaments in the mother-bud neck. *Mol. Cell. Biol.* 7:3678–3687.

Hartwell, L. H. 1980. Mutants of Saccharomyces cerevisiae unresponsive to cell division control by polypeptide mating pheromone. *J. Cell Biol.* 85:811–822.

Hartwell, L. H., J. Culotti, J. R. Pringle, and B. J. Ried. 1974. Genetic control of the cell division cycle in yeast. *Science (Wash. DC).* 183:46–51.

Hasek, J. I. Rupes, J. Svobodova, and E. Streiblova. 1987. Tubulin and actin topology during zygote formation of *Saccharomyces cerevisiae*. *J. Gen. Microbiol.* 133:3355–3363.

Hieter, P., C. Mann, M. Snyder, and R. W. Davis. 1985. Mitotic stability of yeast chromosomes: a colony color assay that measures nondisjunction and chromosome loss. *Cell.* 40:381–392.

Ito, H., Y. Fukuda, K. Murata, and A. Kimura. 1983. Transformation of intact yeast cells treated with alkali cations. *J. Bacteriol.* 153:163–168.

Johnson, D. I., and J. R. Pringle. 1990. Molecular characterization of *CDC42*, a *Saccharomyces cerevisiae* gene involved in the development of cell polarity. *J. Cell Biol.* 111:143–152.

Johnston, M., and R. W. Davis. 1984. Sequences that regulate the divergent GAL1-GAL10 promoter in Saccharomyces cerevisiae. *Mol. Cell. Biol.* 4: 1440–1448.

Karn, J., S. Brenner, and L. Bartnett. 1983. Protein structural domains in the Caenorhabditis elegans unc-54 myosin heavy chain gene are not separated by introns. *Proc. Natl. Acad. Sci. USA.* 80:4253–4257.

Katti, S. K., D. M. LeMaster, and H. Eklund. 1990. Crystal structure of thioredoxin from *Escherichia coli* at 1.68 A resolution. *J. Mol. Biol.* 212:167–184.
Kilmartin, J. V., and A. E. M. Adams. 1984. Structural rearrangements of tubulin and actin during the cell cycle of the yeast Saccharomyces. *J. Cell Biol.* 98:922–933.
Kilmartin, J. V., B. Wright, and C. Milstein. 1982. Rat monoclonal antitubulin antibodies derived by using a new nonsecreting rat cell line. *J. Cell Biol.* 93:576–582.
Knapp, B., M. Rentrop, J. Schweizer, and H. Winter. 1986. Nonepidermal members of the keratin multigene family: cDNA sequences and in situ localization of the mRNAs. *Nucleic Acids Res.* 14:751–763.
Konopka, J. B., D. D. Jenness, and L. H. Hartwell. 1988. The C-terminus of the S. cerevisiae α-pheromone receptor mediates an adaptive response to pheromone. *Cell.* 54:609–620.
Krieg, T. M., M. P. Schafer, C. K. Cheng, D. Filpula, P. Flaherty, P. M. Steinert, and D. R. Roop. 1985. Organization of a type I keratin gene. *J. Biol. Chem.* 260:5867–5870.
Landschulz, W. H., P. F. Johnson, and S. L. McKnight. 1988. The leucine zipper: a hypothetical structure common to a new class of DNA binding proteins. *Science (Wash. DC).* 240:1759–1764.
Lees, J. F., P. S. Shneidman, S. F. Skuntz, M. J. Carden, and R. A. Lazzarini. 1988. The structure and organization of the human heavy neurofilament subunit (NF-H) and the gene encoding it. *EMBO (Eur. Mol. Biol. Organ.) J.* 7:1947–1955.
Marchuk, D., S. McCrohon, and E. Fuchs. 1985. Complete sequence of a gene encoding a human type I keratin: sequences homologous to enhancer elements in the regulatory region of the gene. *Proc. Natl. Acad. Sci. USA.* 82:1609–1613.
Molina, M. I., K. E. Kropp, J. Gulick, and J. Robbins. 1987. The sequence of an embryonic myosin heavy chain gene and isolation of its corresponding cDNA. *J. Biol. Chem.* 262:6478–6488.
Noble, M., S. A. Lewis, and N. J. Cowan. 1989. The microtubule binding domain of microtubule-associated protein MAP1B contains a repeated sequence motif unrelated to that of MAP2 and Tau. *J. Cell Biol.* 109:3367–3376.
Ohya, Y., S. Miyamoto, Y. Ohsumi, and Y. Anraku. 1986*a*. Calcium sensitive cls4 mutant of Saccharomyces cerevisiae with a defect in bud formation. *J. Bacteriol.* 165:28–33.
Ohya, Y., Y. Ohsumi, and Y. Anraku. 1986*b*. Isolation and characterization of Ca^{+2}-sensitive mutants of Saccharomyces cerevisiae. *J. Gen. Microbiol.* 132:979–988.
Pearson, W. R. 1990. Rapid and sensitive sequence comparison with FASTP and FASTA. *Methods Enzymol.* 183:63–98.
Pearson, W. R., and D. J. Lipman. 1988. Improved tools for biological sequence comparison. *Proc. Natl. Acad. Sci. USA.* 85:2444–2448.
Pringle, J. R., and L. H. Hartwell. 1981. The *Saccharomyces cerevisiae* cell cycle. *In* The Molecular Biology of the Yeast Saccharomyces: Life Cycle and Inheritance, Strathern, J. N., E. W. Jones, and J. R. Broach, editors. Cold Spring Harbor Laboratory, Cold Spring Harbor, NY. 97–142.
Rose, M. D., and G. R. Fink. 1987. *KAR1*, a gene required for function of both intranuclear and extranuclear microtubules in yeast. *Cell.* 48:1047–1060.
Rothstein, R. J. 1983. One-step gene disruption in yeast. *Methods Enzymol.* 101:202–211.
Sambrook, J., E. F. Fritsch, and T. Maniatis. 1989. Molecular Cloning: A Laboratory Manual. Cold Spring Harbor Laboratory, Cold Spring Harbor, NY. 545 pp.
Sanger, F., S. Nicklen, and A. R. Coulson. 1977. DNA sequencing with chain-terminating inhibitors. *Proc. Natl. Acad. Sci. USA.* 74:5463–5467.
Shenoy, S., J.-K. Choi, S. Bagrodla, T. D. Copeland, J. L. Maller, and D. Shalloway. 1989. Purified maturation promoting factor phosphorylates $pp60^{c-src}$ at the sites phosphorylated during fibroblast mitosis. *Cell.* 57:763–774.
Sherman, F., G. Fink, and J. Hicks. 1986. Methods in Yeast Genetics. Cold Spring Harbor Laboratory, Cold Spring Harbor, NY. 186 pp.
Snyder, M. 1989. The SPA2 protein of yeast localizes to sites of cell growth. *J. Cell Biol.* 108:1419–1429.
Snyder, M., and N. Davidson. 1983. Two gene families clustered in a small region of the *Drosophila* genome. *J. Mol. Biol.* 166:101–118.
Snyder, M., and R. W. Davis. 1988. *SPA1*: a gene important for chromosome segregation and other mitotic functions in S. cerevisiae. *Cell.* 54:743–754.
Teem, J., N. Abovitch, N. F. Kaufer, W. F. Schwindinger, J. R. Warner, A. Levy, J. Woolford, R. J. Leer, M. M. C. van Raamsdonk-Duin, W. H. Mager, R. J. Planta, L. Schultz, J. D. Friesen, H. Fried, and M. Rosbash. 1984. A comparison of yeast ribosomal protein gene DNA sequences. *Nucleic Acids Res.* 12:8295–8312.
Trueheart, J., J. D. Boeke, and G. R. Fink. 1987. Two genes required for cell fusion during yeast conjugation: evidence for a pheromone induced surface protein. *Mol. Cell. Biol.* 7:2329–2334.
Watzele, M., F. Klis, and W. Tanner. 1988. Purification and characterization of the inducible a glutinin of *Saccharomyces cerevisiae*. *EMBO (Eur. Mol. Biol. Organ.) J.* 7:1483–1488.
Yanisch-Perron, C., J. Vieira, and J. Messing. 1985. Improved M13 phage cloning vectors and host strains: nucleotide sequences of the M13mp18 and pUC19 vectors. *Gene.* 33:103–119.